ORIGINAL ARTICLE

Consequences of vertical basic wood density variation on the estimation of aboveground biomass with terrestrial laser scanning

Miro Demol[1,2] · Kim Calders[1] · Sruthi M. Krishna Moorthy[1] · Jan Van den Bulcke[3] · Hans Verbeeck[1] · Bert Gielen[2]

Abstract

Key message **Stump-to-tip trends in basic wood density complicate the conversion of tree volume into aboveground biomass. We use 3D tree models from terrestrial laser scanning to obtain tree-level volume-weighted wood density.**

Abstract Terrestrial laser scanning (TLS) is used to generate realistic 3D tree models that enable a non-destructive way of quantifying tree volume. An accurate value for basic wood density is required to convert tree volume into aboveground biomass (AGB) for forest carbon assessments. However, basic density is characterised by high inter-, intra-species and within-tree variability and a likely source of error in TLS-derived biomass estimates. Here, 31 adult trees of 4 important European timber species (*Fagus sylvatica*, *Larix decidua*, *Pinus sylvestris*, *Fraxinus excelsior*) were scanned using TLS and then felled for several basic wood density measurements. We derived a reference volume-weighted basic density (ρ_{w}) by combining volume from 3D tree models with destructively assessed vertical density profiles. We compared this to basic density retrieved from a single basal disc over bark (ρ_{bd}), two perpendicular pith-to-bark increment cores at breast height (ρ_{ic}), and sourcing the best available local basic wood density from publications. Stump-to-tip trends in basic wood density caused site-average woody AGB estimation biases ranging from -3.3 to $+7.8\%$ when using ρ_{bd} and from -4.1 to $+11.8\%$ when using ρ_{ic}. Basic wood density from publications was in general a bad predictor for ρ_{w} as the bias ranged from -3.2 to $+17.2\%$, with little consistency across different density repositories. Overall, our density-attributed biases were similar to several recently reported biases in TLS-derived tree volume, leading to potentially large compound errors in biomass assessments with TLS if patterns of vertical basic wood density variation are not properly accounted for.

✉ Miro Demol
miro.demol@uantwerpen.be

[1] CAVElab, Computational and Applied Vegetation Ecology, Department of Environment, Faculty of Bioscience Engineering, Ghent University, Coupure Links 653, 9000 Ghent, Belgium

[2] PLECO, Plants and Ecosystems, Faculty of Science, Antwerp University, Universiteitsplein 1, 2610 Wilrijk, Belgium

[3] UGent-Woodlab, Laboratory of Wood Technology, Department of Environment, Faculty of Bioscience Engineering, Ghent University, Coupure Links 653, 9000 Ghent, Belgium

Introduction

One of the main challenges in estimating forest carbon stocks is to reliably quantify the aboveground biomass (AGB) of standing trees. Commonly, practically measurable tree properties such as tree diameter and height are collected in forest inventories, and used in allometric scaling equations (ASEs) to estimate volume and AGB. Though ASEs have become a popular tool for a wide spectrum of forest monitoring applications, they also feature several inherent weaknesses related to poor representativeness and flexibility (Somogyi et al. 2007; Kearsley et al. 2013; Stephenson et al. 2014). At the same time, a better accuracy of forest AGB is required in, for instance, REDD+ initiatives and for the better understanding of the carbon cycle (Campioli et al. 2016).

Terrestrial laser scanning (TLS) is an alternative technique for estimating the standing volume of individual trees. TLS captures extremely detailed 3D point clouds of the forest environment with unprecedented spatial accuracy. Various modelling techniques have been developed to realistically reconstruct the shape of trees from point cloud data (Pfeifer et al. 2004; Dassot et al. 2012; Hosoi et al. 2013; Raumonen et al. 2013; Hackenberg et al. 2015a), from which total tree volume can be derived. Several validation studies have shown good agreement of TLS-derived volume estimates with destructively assessed volumes, even for large tropical trees (Calders et al. 2015; Hackenberg et al. 2015b; Momo Takoudjou et al. 2017; Saarinen et al. 2017; Gonzalez de Tanago et al. 2018). TLS-calibrated ASEs could eliminate the need for labour-intensive destructive biomass sampling campaigns (Lau et al. 2019). The envisaged further developments in scanning technology and point cloud processing algorithms have the potential to provide massive-scale reliable tree volume data.

Basic wood density is the crucial conversion factor to transform TLS-derived tree volume into AGB and is often calculated as the ratio of mass at 0% moisture content (oven-dry at 103 °C) to the fresh volume of a representative wood sample (Williamson and Wiemann 2010). However, basic wood density is characterised by high variability across species (Chave et al. 2006; Macfarlane 2020), within species (Bouriaud et al. 2004; Martínez-Sancho et al. 2020; Vieilledent et al. 2018), and even vertically and radially within individual trees (Nogueira et al. 2008; Wassenberg et al. 2015; Longuetaud et al. 2017; Bastin et al. 2018). Only limited generalisations about the patterns of variation in density are well described (Wiemann and Williamson 2014).

Ideally, an average basic wood density of different aboveground parts of a tree should be used to convert tree volume into AGB. For example, Sagang et al. (2018) established a tree-specific volume-weighted average basic wood density to convert TLS volume estimates of tropical trees into AGB. To achieve this, trees were felled and the dimensions and density was measured at various locations along the length of the trees. Given the time and effort required to collect such extensive datasets, only few such datasets exist, often describing only a handful of trees. As a result, sample extraction on standing trees is often limited to small-sized samples at easily accessible point of measurement such as at breast height. The most common sample extraction technique that is currently in practice is increment coring due to its relatively non-destructive nature as opposed to the basal disc extraction at breast height (Wiemann and Williamson 2012). When sampling or felling is simply not possible, as is often the case, researchers and forest managers rely on earlier published work in wood density repositories (Zanne et al. 2009; Falster et al. 2015; Martínez-Sancho et al. 2020) or unpublished locally established representative density

data. Many tree species show substantial stump-to-tip and pith-to-bark trends in specific wood density, which is closely intertwined with tree life history strategies and functional type (Momo et al. 2020; MacFarlane 2020), further complicating the accurate quantification of weighted basic wood density. To some extent, pragmatic sampling rules have been established to approximate weighted basic wood density from a single measurement (Wahlgren and Fassnacht 1959; Wiemann and Williamson 2012; Bastin et al. 2015; Wassenberg et al. 2015; Momo et al. 2020), the reliability of such density estimates remains uncertain. Furthermore, as TLS systems capture the whole 3D structure of objects, the resulting tree volume includes bark, whereas basic density measurements often exclude any bark tissues.

The rapidly increasing amount and quality of tree volume data from three-dimensional data-acquisition platforms calls for a reconsideration of basic wood density as a conversion factor. Whereas the uncertainty on TLS-derived estimates of volume is further reduced, the discrepancy between either published or sampled basic density and the average density of the entire (aboveground parts of a) tree is an understudied but likely substantial contributor to errors in AGB estimates with TLS (Momo et al. 2020). For now, it remains unclear what the impact of basic wood density is on the overall uncertainty of AGB estimations from TLS, nor do we know the best strategies to constrain such errors (Disney et al. 2018).

In this study, we specifically focus on the errors on the site-level TLS-derived AGB estimations emanating from within-tree vertical basic wood density variation. Our objectives are (i) to quantify the vertical density variation in 31 adult trees; (ii) to derive volume-weighted basic density for individual trees with detailed TLS tree models and vertical density profiles; (iii) to quantify the density-attributed bias in AGB when converting TLS volumes with common basic density sampling methods and several published basic wood density data sources. Unlike the previous studies focussing on tropical trees, our study focusses on four of the most abundant and commercially important species of Europe.

Materials and methods

We conducted this study in five even-aged and mono-specific managed forest stands in Belgium (Table 1), covering four common European tree species: Scots pine—*Pinus sylvestris* at two sites (referred to as *P.sylA* and *P.sylB*), and one site each of common ash—*Fraxinus excelsior* (*F.exc*), common beech—*Fagus sylvatica* (*F.syl*) and larch—*Larix decidua* (*Lx.dc*). At all sites, a medium–heavy thinning-from-below was scheduled for 2018 in accordance with the forest management plan, except for *F.exc*, which had an emergency sanitary clearcut due to ash dieback (*Hymenoscyphus*

Table 1 Site characteristics and scanning settings at the five mono-specific, even-aged forest stands where the experiments took place

| Site	Municipality	Latitude	Longitude	Species	Understory	Age (years)	Soil type	TLS	Foliage
P.sylA	Brasschaat	51.31	4.55	*Pinus sylvestris*	*Molinia caerulea*	74	Gleyic podzol	VZ-1000	Needle
P.sylB	Louvain-la-Neuve	50.68	4.60	*Pinus sylvestris*	Absent	~58	Albic podzol	VZ-1000	Needle
Lx.dc	Oostkamp	51.12	3.19	*Larix decidua*	Absent	33	Albic podzol	VZ-400	Needle-off
F.syl	Wuustwezel	51.39	4.55	*Fagus sylvatica*	Absent	~107	Albic podzol	VZ-1000	Leaf-off
F.exc	Bever	50.72	3.96	*Fraxinus excelsior*	*Sambucus nigra*	33	Fluvic gleyic phaeozem	VZ-1000	Leaf-off

Age: average tree age at breast height determined from year-ring counting along a radial transect on a finely sanded cross-sectional stem disc. A ~ indicates that the number of counted rings differed between individual trees. In this case, the maximum ring count was taken to represent stand age of the even-aged stands. TLS: Type of RIEGL VZ-series terrestrial laser scanning instrument used for data collection. Foliage: leaves or needles present ('Needle') or absent ('Needle-off', 'Leaf-off') during scanning

fraxineus). The forest manager selected the individuals for thinning; from these, we randomly selected five (six for *P.sylB* and ten for *F.exc*) target trees in five equidistant tree diameter classes spanning the stand diameter range. As a result, we used a total of 31 target trees in the experiment.

## Terrestrial laser scanning and point cloud processing

All five stands were scanned using a RIEGL VZ-1000 or VZ-400 time-of-flight near-infrared terrestrial laser scanner between Dec 2017 and March 2018, at a pulse repetition rate of 300 kHz, beam divergence of 0.35 mrad and an angular sampling resolution of 0.04°, in both horizontal and vertical directions. The data resulting from the two instruments are intercomparable, as there are no differences in their XYZ measurement accuracy (Calders et al. 2017). We used anywhere between 9 and 20 scan positions per site, forming a squared grid-like pattern with 20 m length. A 10 m buffer distance between the target trees and the grid's outer border was maintained throughout (Fig. 1). During the scanning, wind speeds were consistently less than 2 Bft and there was no precipitation. A scanning pattern as suggested in Wilkes et al. (2017) was followed, where consecutive scans formed a continuous chain along the positions. We minimised occlusion by scanning in winter under leaf-off conditions for the broadleaved and larch trees (Table 1).

The single scans were coregistered using the scanner manufacturer's processing software RiSCAN PRO. We used *treeseg* (Burt et al. 2018) to semi-automatically segment the 31 target trees from the plot-level point clouds of different sites (Fig. 2a). All single tree point clouds were then filtered for pulse shape deviation < 20 and reflectance > − 10 dB (Calders et al. 2017). For *Lx.dc*, which was scanned with a VZ400 instrument, we filtered on deviation < 12 and reflectance > − 17 dB, which produced very similar spectral properties in the point cloud. Additionally, point clouds were filtered with a maximum range of 45 m from the scanner
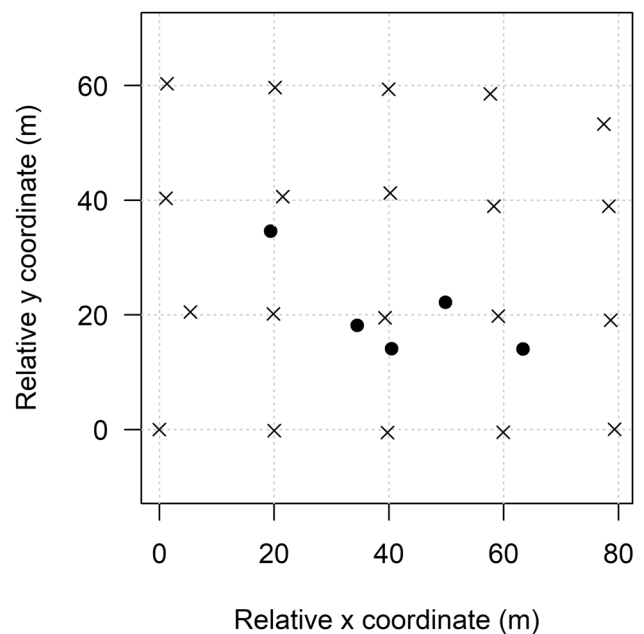
Fig. 1 Scan position layout at *F.syl*. Scan positions (crosses) formed an approximately 20 m squared grid. The number of scan positions was taken large enough to contain the stems of the target trees (bullets) while maintaining a distance of at least 10 m between the outer margins of the grid and the target trees

origin to reduce the adverse effects of noise, suboptimal coregistration results and branch movements, on the point cloud quality. Filtered point clouds were then downsampled with a voxel grid centroid filter to have a point spacing of 10 mm or 15 mm. From the single tree point clouds, tree height was calculated as the difference in *z*-coordinate between the highest and lowest 3D point. The Quantitative Structure Model (QSM) algorithm *treeQSM* version 2.3 (Raumonen et al. 2013) was used to estimate the total tree volume by building cylindrical models of the tree structure. *treeQSM* is stochastic in nature with identical input parameters producing slightly different QSMs with different runs.
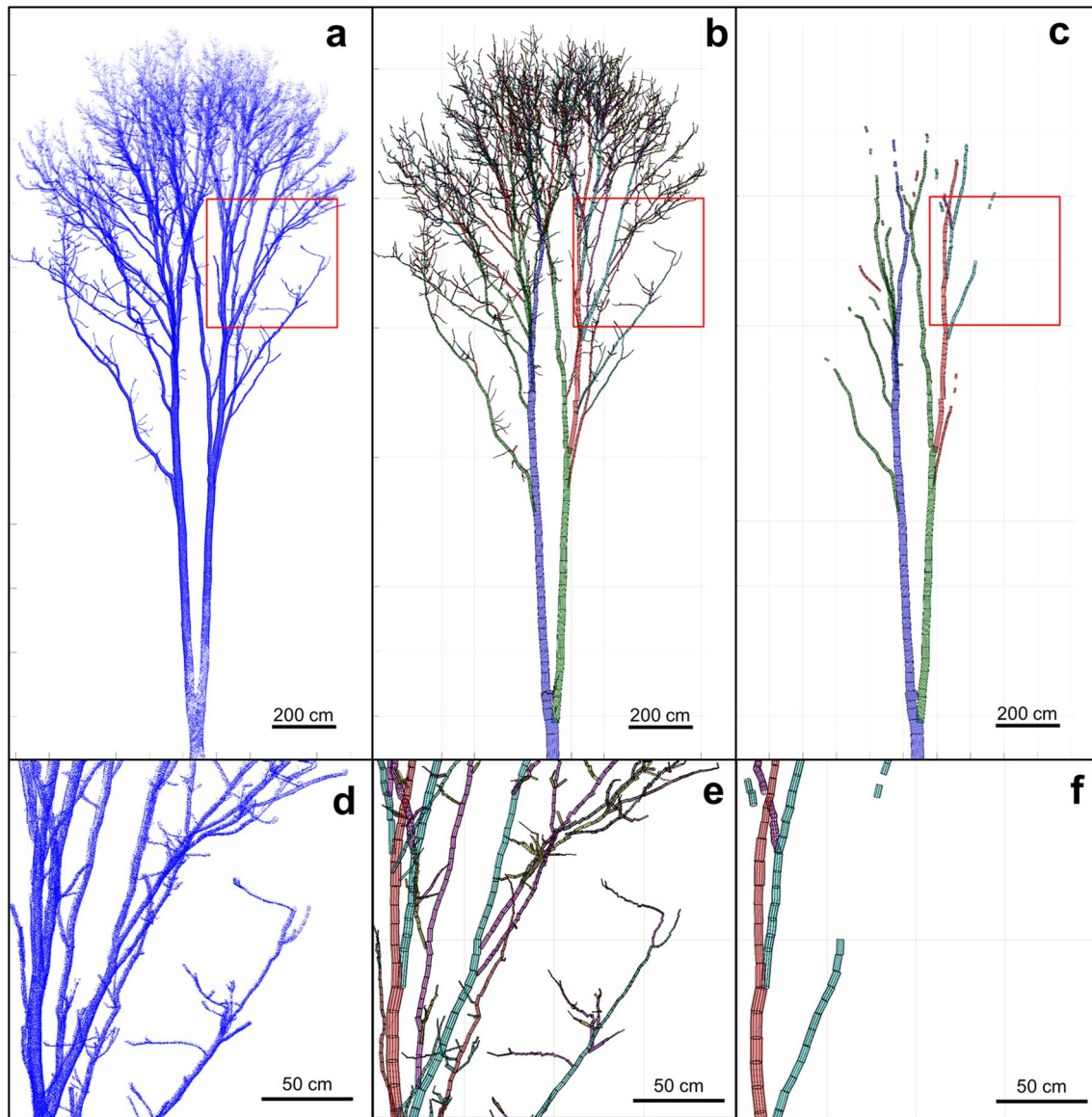
Fig. 2 Example point cloud and (coarse) woody volume reconstructions of a 23 m tall common ash tree (Fraxinus excelsior). Point cloud obtained with a RIEGL VZ-1000 laser scanner. **a** Segmented, filtered and downsampled pointcloud. **b** One quantitative structure model (QSM) reconstruction using the optimised input parameters. **c** The reconstructed coarse woody volume applying a 7 cm threshold for cylinder diameters on the original QSM in (**b**). **d**–**f** are magnifications of the red square in (**a**), (**b**), (**c**), respectively

As *treeQSM* requires optimisation of input parameters, we computed QSMs over a range of realistic input parameter combinations, and made ten replications for each combination. In total, 70 models were constructed per tree point cloud. The optimal parameter combination was selected based on a minimisation of the mean point-model distance. The mean tree volume of the ten best models with identical input parameters was calculated and the QSM with total tree volume closest to this mean was retained for further analyses (Fig. 2b). We were unable to accurately model the diameters of fine branches and needles (smaller than around 5 cm in diameter), and QSMs caused large volume overestimations of the tree crowns (Supp. Fig. 3). Earlier studies validating the TLS-derived tree volume using the same scanner and scanning setup (e.g. Hackenberg et al. 2015a; Momo Takoudjou et al. 2017; Lau et al. 2018) have shown that TLS accurately estimated the volume of all woody parts larger than 7 cm in diameter. Therefore, we removed all QSM cylinders with diameter < 7 cm diameter in all further analyses. The quality and accuracy of the automatically optimised QSMs were evaluated with destructive diameter, tree height and stem volume measurements (Supp. Figure 1, 2, 3).

Forest inventory and destructive sampling

For each target tree, we measured total tree height, height of the first living primary branch with a diameter > 5 cm with a Nikon Forestry Pro laser rangefinder, and the circumference over bark at 130 cm (converted to diameter at breast height (DBH) assuming a cylindrical bole) with measurement tape. We took increment cores at breast height in two perpendicular directions with a 5.15 mm diameter Haglöf extractor, aiming to extract two full pith-to-bark (excluding the bark itself) cores. The wood samples were immediately packed in plastic straws to prevent water loss.

Trees were felled as close as possible to the ground. DBH, tree length and tree length at first living branch were remeasured with measuring tape. We prefer to use the term length rather than height here, as it was measured on felled trees. We then split the tree into two parts: stem part (below the first living branch > 5 cm diameter) and crown part (above the first living branch > 5 cm diameter). The fresh weight of each of these parts was weighed immediately after felling using a Dynafor LLX1 dynamometer (capacity 1000 kg, precision 0.5 kg), and lifted with a crane, tripod or hoist attached to a tree. Cross-sectional discs of ~ 5 cm thickness were sampled from the main stem with a chainsaw at following lengths: at breast height (130 cm) and every 300 cm (at 300, 600, 900, 1200 cm, …) until the tree top was reached. At the *P.sylB* site, discs were extracted at multiples of 315 cm height (315, 630, 945 cm, and not at breast height, in accordance with the local logging contract requiring logs of at least 300 cm. At the *Lx.dc* site, an additional stump disc at 40 cm height was taken. As these heights were fixed, some discs featured deformities like knots or forks. The relative height of the discs was obtained by dividing the absolute sampling height by the total tree length. All discs were immediately packed in plastic bags to prevent water loss.

Lab basic wood density measurements

The discs were transported to the lab, cleaned with compressed air to remove loose bark, dirt, moss and lichens, and weighed to a precision of 1 g (or 0.01 g for samples < 350 g weight) on the day of sampling itself. The fresh volume of the discs including bark was measured using the Archimedes water displacement method (Williamson and Wiemann 2010). For this, the samples were fully submerged into an open water container placed on a top-loading 15 kg capacity balance (1 g precision). The weight readings were interpreted as volume as we assumed the density of water to be 1000 g l^{-1} and water absorption into the discs negligible. Two pieces were cut from each increment core: one inner section from the pith to halfway the radius, and one outer section from halfway the radius to the cambium (excluding the cambium itself). The cut was made exactly perpendicular

to the core axis with a very sharp knife. The increment core fragments were submerged in water for 24 h. The wet wood volume was then obtained by measuring the length of the core and assuming a cylindrical shape with diameter 5.15 mm corresponding to the inner diameter of the extractor (Schüller et al. 2013). The discs and cores were weighed again to the same precision as above after oven-drying at 103ºC until their weight changed less than 1 g or 0.001 g in 48 h, respectively. The basic wood density of each sample was calculated as the ratio of its oven-dry weight to its fresh volume, in kg m^{-3}. We defined the basic density of the full disc at breast height (or at 315 cm height in *P.sylB*) as the basal basic wood density (referred to as ρ_{bd} throughout the manuscript). The density of the cores was computed by weighing the density of the inner and outer section by their corresponding area assuming a circular tree cross-section. The average density of two perpendicular increment cores, referred to as ρ_{ic} throughout the manuscript, was used.

Volume-weighted basic wood density calculations

We computed the reference volume-weighted basic wood density estimate for each tree (referred to as ρ_w from now on). The QSM approach allowed the explicit location and quantification of the coarse woody volume of all above-ground parts of the scanned trees (Fig. 3). To calculate ρ_w, each QSM cylinder segment was attributed the basic wood density value of the sampled disc with the closest z-coordinate. Cylinders that fell in between two measured wood discs
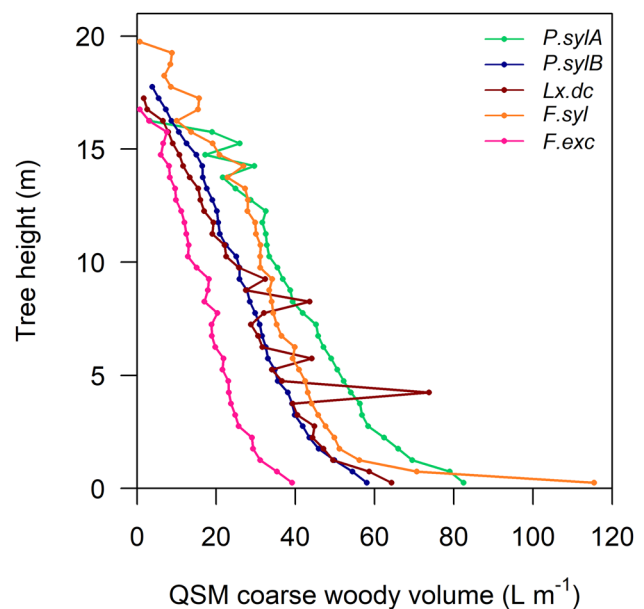
Fig. 3 Vertical quantitative structure model (QSM) coarse woody volume distributions expressed in litre per vertical meter. QSM woody volume was quantified in 50 cm height bins (points). Per site, the tree with median diameter at breast height is represented

were split according to where the z-distance to both adjacent discs was equal and each part got the respective basic wood density value of the closest disc. Coarse wood aboveground biomass (cAGB) was then obtained by summing the AGB of individual cylinders larger than 7 cm in diameter. Then, ρ_w was calculated as cAGB divided by coarse woody volume.

Basic wood density from literature

We adopted two main strategies to search for basic wood density matching the geographical location and species used in this study as close as possible. First, the Global Wood Density Database (GWDD; https://doi.org/10.5061/dryad.234 (Zanne et al. 2009)) was queried for species level matches (genus level matches for *Larix decidua*) of basic wood density observations in Europe. Additionally, we compiled increment coring basic wood density data from GenTree Database (Martínez-Sancho et al. 2020). We filtered for records from Belgium's neighbouring countries as GenTree had no Belgian observations. Second, we searched for destructive basic wood density measurement experiments in Belgium (ρ_{Be}). See Table 2 for an overview of the different basic wood density sources.

Statistics

The variation of vertical wood density within-tree and among individuals was computed as (min–max)/mean. Loess smoothers were used to get vertical basic wood density profile averages per tree species and site. Bias

in coarse AGB (cAGB) estimates were computed as $(cAGB_{proxy} - cAGB_{vw})/cAGB_{vw}$ for single trees and as $(\sum(cAGB_{proxy,i} - cAGB_{vw,i})/\sum(cAGB_{vw,i})$ for a site-average bias, with $cAGB_{proxy}$ being the cAGB estimated with ρ_{bd}, ρ_{ic}, and ρ_{Be}, $cAGB_{vw}$ being the reference cAGB computed with volume-weighted basic density ρ_w, and i being the sampled trees in each site. We tested for differences in mean basic wood density per site across different sampling techniques with a paired t test after checking for normality with a Shapiro–Wilk test. Statistical data processing and visualisations were prepared in R (R Development Core Team 2011).

Results

Basic wood density comparison

For every site and species, six different basic wood density sources were compared in this study: three from wood sampling and three from reference publications or repositories (Table 2). First, we were able to extract at least one European basic wood density entry for all species in GWDD (Zanne et al. 2009), except for *Larix decidua*, where we used a genus level basic wood density. Overall, 1–3 values were withheld for each species or genus from GWDD that could be traced back to the following three original references: Lavers and Moore (1983), Schütt et al. (1994), and Wagenführ and Schreiber (1985). Second, we were able to locate the average basic wood density from the GenTree database for two species of the four species: *P. sylvestris* and *F. sylvatica*

Table 2 General wood and tree characteristics of the target trees

Site	n	DBH (min–max) in cm	Tree length (m)	Sampled basic wood density (kg m^{-3} ± standard deviation)			Reference basic wood density (kg m^{-3} ± standard deviation)		
				Base disc ρ_{bd}	Increment coring ρ_{ic}	Weighted ρ_w	Belgian ρ_{Be}	GenTree	GWDD
P.sylA	6	30.9 (25.1–36.3)	21.0	488 ± 16	504 ± 36	452 ± 17	502[d]	461 ± 63	422
P.sylB	5	30.8 (18.1–44.1)	23.4	444 ± 29[a]	466 ± 34	432 ± 18	502[d]	461 ± 63	422
Lx.dc	5	27.4 (23.6–32.1)	20.6	500 ± 19	487 ± 27	488 ± 14	474 ± 51[e]	No data	429[b]
F.syl	5	31.0 (26.1–37.7)	21.8	565 ± 11	563 ± 12	551 ± 14	550 ± 12[c]	597 ± 52	585
F.exc	10	21.8 (11.5–35.3)	18.6	553 ± 28	551 ± 25	566 ± 25	523 ± 34[c]	No data	560

n: number of scanned and harvested trees. DBH: diameter over bark at breast height. Tree length: average length along the main axis of the felled tree. Sampled basic wood density: basic wood density obtained from increment cores (average of two perpendicular cores at breast height) ρ_{ic}, a full cross-sectional base disc including bark ρ_{bd}, and a vertically resolved volume-weighted average ρ_w (refer to the method section for a full description). Reference basic wood density: basic wood density extracted from various destructive experiments in Belgium (ρ_{Be}), GenTree (Martínez-Sancho et al. 2020) for observations in France and Germany, and the Global Wood Density Database (Zanne et al. 2009) filtered on values for Europe. Values are reported with standard deviation if available. ρ_{Be}

[a] For *Lx.dc*, a genus level database value was used averaging the basic wood density of *L. decidua, L. kaempferi* and *L. eurolepis*

[b] For *P.sylB*, no breast height disc was sampled, but a disc at 315 cm height was used

[c] Vande Walle (2007

[d] Janssens et al. (1999

[e] cited in Vande Walle et al. (2005)

(Martínez-Sancho et al. 2020). The average basic wood density was 461 kg m^{-3} from 103 increment core samples for *Pinus sylvestris* and 597 kg m^{-3} from 201 increment core samples for *Fagus sylvatica*. These observations were made from trees in France and Germany with an average age and DBH of 102 years and 42 cm for *P. sylvestris* and 134 years and 43 cm for *F. sylvatica*. GenTree did not have entries for the other species. Finally, a Belgian reference basic wood density ρ_{Be} for each site was found in Janssens et al. (1999), Vande Walle et al. (2005), and Vande Walle (2007). For each species and site, these three sets of published basic wood density data differed less than 50 kg m^{-3} from each other, except for the GWDD value for *P. sylvestris*, which was 40 kg m^{-3} and 80 kg m^{-3} lower than the GenTree and Belgian value, respectively.

Basal basic density showed the highest variation at the Scots pine stand in *P.sylB*, ranging up to 16% for ρ_{bd} and 18% for ρ_{ic}. The other Scots pine stand *P.sylA* showed only slightly less variation (8.5% and 18% for ρ_{bd} and ρ_{ic}, respectively) and had a smaller DBH range as compared to *P.sylB* (Table 1). The broadleaved stands *F.syl* and *F.exc* had a basic wood density variation of 5% for ρ_{bd} and 14% for ρ_{ic}. At *Lx.dc* density varied the least, by 8% 13% for ρ_{bd} and ρ_{ic}, respectively. This was also the most homogeneous site in

terms of DBH and tree height ranges. The conifers had a lower basal basic density than the broadleaves. The slightly older but smaller *P. sylvestris* trees at *P.sylA* had a higher ρ_{bd} and ρ_{ic} than *P.sylB*.

On average, increment coring method gave similar basic wood density values than the basal disc method, with absolute differences ranging from -75 to 52 kg m^{-3} for individual trees (Table 2). The largest differences per site between both methods were observed in the coniferous sites. In *Lx. dc* increment coring, densities were on average 2.6% lower, in contrast, at *P.sylA* and *P.sylB* increment coring gave on average 3.2% and 5.5% higher densities. The *F.exc* and *F.syl* stands showed an average ρ_{ic} that was 0.3% and 0.2% lower than ρ_{bd}. We found no evidence that these differences were significantly different from zero using a two-sample *T* test. The difference between inner and outer density was largest in *Lx.dc;* outer wood was on average 51 kg m^{-3} heavier than inner wood. The difference between inner and outer wood at the other sites was less than 5 kg m^{-3} (Supp. Figure 4).

Vertical trends in basic wood density

All species showed a general decrease in basic wood density from stump-to-tip, except for *F.exc*, which had the
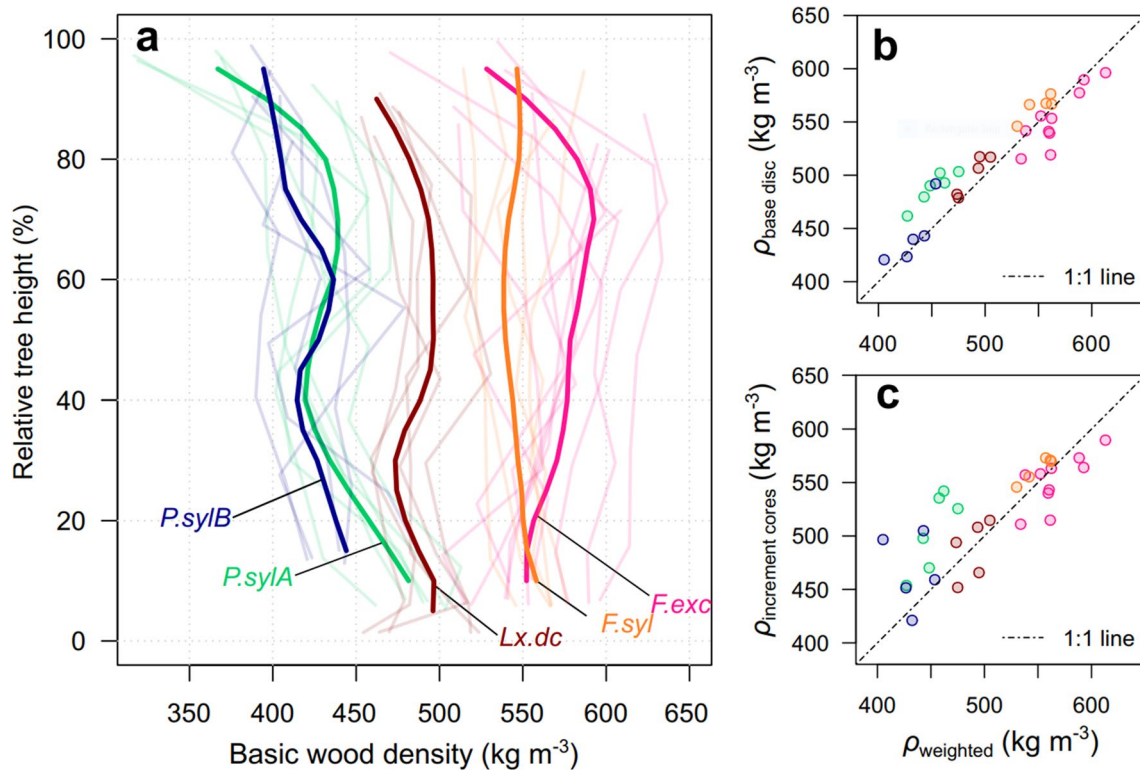
Fig. 4 Basic wood density distributions in 31 destructively sampled trees at five sites in Belgium. **a** Basic wood density sampled from full cross-sectional discs along the main axis of the tree. An average trend per site is represented with a loess smoother (full line). **b** Comparison between volume-weighted basic wood density ρ_w and basal basic density from a single disc measurement ρ_{bd} (same colour coding as (**a**)). **c** Comparison between ρ_w and basic density from two area-weighted perpendicular increment cores at breast height ρ_{ic}

highest densities at a relative tree height of around 0.7 for most individuals (Fig. 4). At this height, basic wood density was on average 7% higher than ρ_{bd}. The vertical trend was the most pronounced for the Scots pine stands (at *P.sylA* from 481 kg m^{-3} at breast height to 367 kg m^{-3} at the highest disc, for *P.sylB* from 444 to 394 kg m^{-3}, respectively). The larch trees at *Lx.dc* did not show a clear trend in the average vertical basic wood density profile, except for slightly lower densities at relative tree heights of 0.3 and 0.8. The trees at *F.syl* site displayed a smooth weakly negative density trend from breast height to ~ 0.6 relative tree height (from 558 to 538 kg m^{-3}), with the highest branches having intermediate densities (546 kg m^{-3}).

Quantifying the vertical trends in basic wood density at the level of the individual tree coupled to highly detailed QSM reconstructions allowed the calculation of a volume-weighted basic density ρ_w. The base disc basic wood density ρ_{bd} was higher than the volume-weighted basic wood density at *P.sylA*, *Lx.dc*, and *F.syl,* whereas no difference could be detected at *P.sylB* and *F.exc* (Student's t test (Fig. 4b and c, Table 2). Similarly, basic density from increment coring ρ_{ic} was generally equal or higher than weighted basic wood density at all sites except at *F.exc*. Here, ρ_{ic} was slightly lower than ρ_w. Basic wood density from local sources (ρ_{Be}) differed more ambiguously from weighted basic density.

Quantifying aboveground biomass

Different basic wood density estimates either under or over-estimated the whole-tree volume-weighted basic wood density. As a result, these basic wood density estimates inevitably introduced bias when they were used for converting TLS-derived volume to AGB (Fig. 5). For individual trees, using ρ_{bd} caused a cAGB bias between −7.5 and 9.7%, compared to between −7.3 and 22% for increment coring and

Fig. 5 Basic wood density attributed bias in coarse wood aboveground biomass (cAGB) estimation of single trees at five sites in Belgium with respect to using volume-weighted basic wood density ρ_w. cAGB was computed from the terrestrial laser scanning derived coarse woody volume and (1) basal disc basic wood density ρ_{bd} (white boxes), (2) average basic wood density from two perpendicular increment cores ρ_{ic} (dark grey boxes) and, (3) published Belgian basic wood density values ρ_{Be} (light grey boxes). In *P.sylB*, the base disc was not sampled at breast height, but at 315 cm height. Percentages on the left-hand indicate site-specific cAGB bias. Asterisks indicate the significances of a one-sample Student t-test on pooled individual tree data (unweighted)
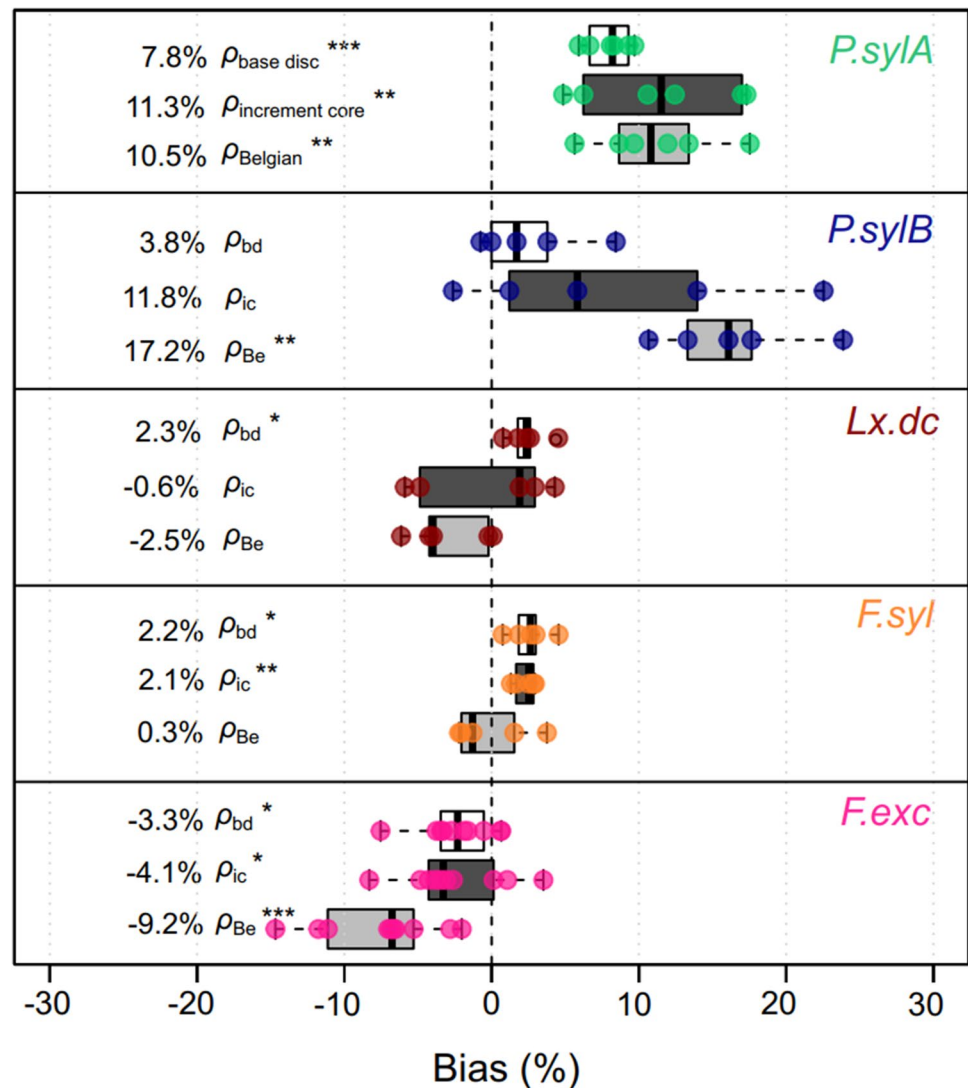
between −14.7 and 23.9% when using local wood density data ρ_{Be}. Simple linear regressions were used to predict cAGB bias from DBH, yielding no significant trends at any site nor with any basic density alternative.

Across all the sites, the site-average bias in cAGB computed with ρ_{bd} ranged from −3.3 to 7.8% (Fig. 5, left-hand column), but contrasting trends among sites were observed: cAGB was overestimated for the coniferous sites and *F.syl* and underestimated for *F.exc*. The largest bias was observed in *P.sylA*, estimating cAGB 7.8% higher than the reference cAGB. The coring method gave similar results as the base disc method for all sites, except at *Lx.dc* showing a site-average bias in cAGB of −0.5% which was not significant. Finally, using local basic wood densities, cAGB was overestimated at *P.sylA* and *P.sylB* by more than 10% and 17%, respectively. *F.exc* and *Lx.dc* were underestimated by 9.2% and 2.5%, respectively. *F.syl* was nearly unbiased (0.3% overestimation).

Discussion

Overall, the average basic wood density of our trees, irrespective of the extraction method, were within the range of published values (Wagenführ and Schreiber 1985; Zanne et al. 2009; Martínez-Sancho et al. 2020), regardless of the sampling method (Table 2). However, density varied substantially at multiple levels: between trees, across sampling methods, and along tree height. To effectively exploit new 3D tree volume datasets for quantifying forest biomass, an accurate basic wood density of each reconstructed tree is required, or *a minima* an unbiased population average. In the presented study, none of the commonly used methods was able to reliably estimate ρ_w at all the five sites. This strengthens the case for continued investigation of the variation of basic wood density within and among trees as pointed out by Bastin et al. (2015), Momo et al. (2020), Sagang et al. (2018) and Wassenberg et al. (2015). We proved that this is relevant, even for relatively well-studied commercial temperate tree species that are among the most abundant in Europe (Brus et al. 2012).

Vertical and inter-tree variation in basic wood density

The vertically resolved species-specific basic wood density patterns observed in this study (Fig. 2a) corroborate with earlier research. Towards the treetop, basic wood density was either declining (conifers), constant (common beech) or increasing (common ash). It is well documented that most species of *Pinus* and *Larix* sp. feature a decrease in basic wood density at successive heights, for instance, for several North-American pines species (Macfarlane 2020; Wahlgren

and Fassnacht 1959), for *P. massoniana* (Wassenberg et al. 2015), for *P. sylvestris* (Repola 2006), for *Larix* sp. (Barnett and Jeronimidis 2003). This is attributed to an increasing proportion of the lighter corewood towards the tree top (Barnett and Jeronimidis 2003). We did not observe a vertical trend in basic wood density for beech, in agreement with Longuetaud et al. (2017) and Schauvliege (1995). The vertical increase in basic wood density in ash are in line with earlier findings that report heavier branch wood than stem wood (Schauvliege 1995; Le Goff et al. 2004; Alberti et al. 2005). Species-specific trends were also reflected in individual vertical basic wood density profiles, despite occasional outliers caused by e.g. knots (especially in conifers) or partial decay. For instance, ash dieback likely caused the lower densities for the smallest branches, despite only sampling visibly healthy individuals. The majority of samples come from vertically oriented stem parts and branches, as we sliced wood discs only from the main axis of the tree. As a result, we expect heavier wood in more horizontal higher order branches to withstand gravitational forces and. snow loading (Cannell and Morgan 1989).

Species-specific stump-to-tip basic wood density profiles showed parallel trends among individual trees, contrasting with a high inter-tree basal basic wood density variability of up to 25% (Fig. 2a). This might be surprising considering the homogeneity of the forest stands covered in this study (all even-aged, single species, planted and managed forests, trees selected less than 80 m apart). The large inter-tree variance suggests that basic wood density is in a large part controlled by genetic or genetic x environmental interactions, called the 'tree effect' (Bouriaud et al. 2004). This behaviour offers promising opportunities to predict weighted basic wood density from a single basic wood density measurement (high variability) using a species-specific vertical basic wood density profile (low variability) and has been tested in several studies before (Hakkila 1967; Wiemann and Williamson 2012; Bastin et al. 2015; Wassenberg et al. 2015). However, such sampling designs rely on strict assumptions of tree vertical volume distribution (e.g. parabolic or conic, see also Fig. 2b) and linear radial/vertical basic wood density trends and are to be applied with caution. The dataset presented here is perhaps too limited to formulate and test these prediction models.

Basic wood density sampling at breast height

In this study, we included two sampling strategies for obtaining breast height basic wood density: a fully destructive cross-sectional disc including bark for which the tree needs to felled, and a semi-destructive extraction of an increment core that can be performed on living trees. Breast height density differed from weighted basic density ρ_w in accordance with the vertical within-tree density variations

described above (Fig. 2c, Table 2). The densities from the full cross-sectional discs could be viewed as 'true' densities as they represented the entire section of the wood at breast height. The large size of the specimens minimised possible systematic errors (e.g. water absorption during volume measurements with the Archimedes method). This could, however, have been problematic for small wood samples such as fine increment cores. By applying a simple weighing procedure with respect to inner and outer wood area and measuring coring volumes with geometrical principles, this was largely avoided (Williamson and Wiemann 2010; Bastin et al. 2015). This resulted in site-specific ρ_{ic} that were less than 15 kg m^{-3} different from ρ_{bd} for the conifer sites and nearly identical for the broadleaved sites. Pith-to-bark radial basic wood density trends at breast height have been studied for *Fagus sylvatica* (slow increase (Longuetaud et al. 2017), small decrease (Bontemps et al. 2013)), for *Pinus sylvestris* (sharp increase for the first 20–30 growth years, and stabilises in outer rings Lachenbruch et al. 2011; Auty et al. 2014)), and for *Larix* sp. (similar as *P. sylvestris* (Karlman et al. 2005)). In contrast, we only found differences between inner and outer basic wood density for the larch trees at *Lx. dc* of around 50 kg m^{-3} but not for the Scots pines at *P.sylA* and *P.sylB*. Our study shows that applying an area-weighted approach for increment coring can correct for pith-to-bark density variations and that the patterns of variation cannot be assumed to corroborate with published patterns.

The residual difference between ρ_{bd} and ρ_{ic} could be attributed to inclusion of bark in the cross-sectional disc samples, whereas bark was not included in the increment cores. Differences would scale with the proportional bark thickness and will be bigger for species exhibiting a thicker bark or lighter bark or a combination of both. This was not explicitly quantified in the present study and can be an important subject for future investigation. However, as the observed residual densities were small and the proportion of bark was small for the species covered in this study, we assume this effect was close to negligible.

Increment coring is a very useful and popular sampling technique for basic wood density quantifications and dendrochronological research alike. New developments of advanced basic wood density estimation methods, including X-ray computed tomography of increment cores (Van den Bulcke et al. 2019), will likely contribute to constraining density measurement errors from increment cores. Additionally, X-ray computed tomography enables to quantify a radial basic wood density profile, allowing to correct for pith-to-bark basic wood density variation on a finer scale than in this study (Bastin et al. 2015).

Current basic wood density repositories are not suitable to get tree-average basic density

We found three useful basic wood density repositories for our species: the widely used Global Wood Density Database (GWDD, Zanne et al. 2009), the large European increment coring dataset GenTree (Martínez-Sancho et al. 2020) and a compilation of published local basic wood density sources. Whereas GWDD has aided biomass inventories in the tropics substantially, our study shows that it is of limited use for converting TLS-derived tree volume into biomass for European tree species. This is because only a limited amount of wood density data entries were available: at the time of writing, a maximum of two data sources were found per species covered in this study. Moreover, all these entries originated from German and British wood atlases. We could not find any information of the geographical location where the wood samples originated from, or the age/size distribution of the sampled trees. Besides, the cited basic wood density values were measured from ideal sawn timber samples without accounting for the presence of bark, knots, (partial) decay, branchwood, etc., which will alter basic wood density substantially.

GenTree only covers seven tree species but contains over 3000 whole-core pan-European basic wood density measurements. As opposed to GWDD, GenTree allows to subset on e.g. geographical, size, or age characteristics and report basic wood density with a confidence interval (Table 2). We see two shortcomings when using the GenTree database in conjunction with TLS data for biomass inventories: the limited tree species covered, and the reporting of breast height basic density rather than ρ_w.

The limitations of GWDD and GenTree prompted us to query more small-scale, local sources of basic wood density (called 'Belgian' basic wood density, Table 2). We found destructively assessed vertical basic wood density profiles for all species except *Larix* sp. However, a smaller geographical distance was no guarantee for more accurate density estimate. This is exemplified by a difference in basic wood density of > 50 kg m^{-3} between Janssens et al. (1999) and *P.sylA*, sites that are less than 2000 m apart.

The density differences between ρ_w and the density derived from GWDD, GenTree and Belgian local sources were relatively modest (< 50 kg m^{-3} for most sites). However, unlike with using ρ_{ic} or ρ_{bd}, the sign of the error was unpredictable as both over- and underestimations occurred within sites and species. Overall, (semi-)destructive sampling for basic wood density, through increment cores or stem discs, seems inevitable for applications where accuracy is indispensable.

Suboptimal sampling introduces bias in cAGB estimation

Not accounting for vertical trends in basic wood density introduced an error when converting TLS coarse woody volume into cAGB. Aggregated per stand, the bias ranged up to 8% for the ρ_{bd} approximation, up to 11.8% for ρ_{ic} and up to 17.2% when applying the most suitable local density value ρ_{Be} for our particular site. We did not find any evidence for species-specific bias scaling with DBH or tree height, except for *F.exc*, due to the homogenous stand structure and limited sample size, In *F.exc*, larger individuals had a larger relative underestimation in basal basic wood density-derived AGB.

Few other studies have compared approximated basic wood density with the volume-weighted average basic density as it requires accurate density measurements coupled to volume assessments at various locations along the length of the tree. Using TLS, we were able to achieve this in a relatively cost-efficient manner. Our estimates of basic wood density-induced cAGB bias matches the bias in plot-level TLS-derived AGB of 9% reported by Sagang et al. (2018) for a set of 130 trees in Cameroon. Additionally, Longuetaud et al. (2017) found differences of ~5% between basal basic wood density and whole-tree basic wood density for *Abies alba* and *Pseudotsuga menszziesii* but no difference for several common European broadleaved species including *Fagus sylvatica*.

Multiple validation studies till date report stand-level TLS volume prediction errors of −7.3%, +3.6%, +2.8% (Hackenberg et al. 2015b), −3.7% (Gonzalez de Tanago et al. 2018), −0.5% (Stovall et al. 2017), +15.2% (Momo Takoudjou et al. 2017), and biomass prediction errors of +9.7% (Calders et al. 2015), 5.5%, 5.3% (Kankare et al. 2013), reflecting the compound effects of occlusion (volume underestimation) and inflation of fine branches (volume overestimation). An interesting exercise would be to compare the error on AGB estimates attributed to basic wood density on one hand and TLS-QSM volume on the other on the same trees. Nevertheless, no such effort has been undertaken till date. However, synthesizing the above results, we expect a comparable order of magnitude for the basic wood density versus TLS volume errors (both roughly ranging 5–15%), leading to a potentially large compound error on TLS-derived AGB estimates, which warrants further investigation. Point cloud processing algorithms and scanner hardware are continuously improving, progressively reducing the uncertainties in TLS-derived volume estimates (Calders et al. 2020). The effectiveness of TLS for AGB quantification will also require a similar reduction in basic density uncertainty. This will require investigating the potential relationships between local site conditions, genetics, niche plasticity, etc. with basic wood density for many dominant species worldwide.

Structural information from TLS and 3D tree models can play a pivotal role in disentangling the drivers of within-tree variation of wood characteristics (Jackson et al. 2019) and is promising for the quantification of volume-weighted traits using explicit volume distributions (Fig. 2b). However, several shortcomings remain, such as the problematic modelling of fine branches. Here, we did not account for thin woods (all tree parts < 7 cm diameter) which typically hold between 10 and 20% of the total tree volume (Dieter and Elsasser 2002; Vallet et al. 2006) in temperate or 7–14% (Gonzalez de Tanago et al. 2018) in tropical adult trees. Also, the vertical binning to assign a basic wood density value to every QSM segment is a rather crude simplification of the full variability of basic wood density throughout the tree, as is taking wood samples only every 300 cm along the main stem. Nevertheless, the results presented here still advocate for carefully considering the potentially large variation that is hidden behind a single basic wood density value.

Conclusions

The advent of TLS in forest ecology has been motivated by the potential of TLS to reliably estimate the volume of standing trees. Basic wood density, which is used to convert tree volume into biomass, shows high- and multi-dimensional variability. However, sampling entire trees to quantify intra-individual basic wood density as performed in this study is extremely time-consuming and, therefore, is rarely done for practical applications. Multiple legal, social and scientific constraints often inhibit the destructive sampling of trees. Relying upon approximated basic wood density values is often the only pragmatic way of getting a sensible density estimate.

Here, we showed that approximations in basic wood density significantly contribute to the error in estimating coarse wood AGB (cAGB) from TLS data for four of the most widespread timber species across Europe. cAGB computed with basal basic wood density (from increment coring and full discs at breast height) was overestimated for the conifers and common beech due to a negative stump-to-tip trend in basic wood density, and underestimated for common ash. Basal disc and increment coring basic wood density induced a stand-specific bias ranging −3.3 to 7.8% and −4.1 to 11.8%, respectively. Basic density inferred with geometrical principles from increment coring provides a nondestructive way to approximate the density of a full disc. Basic wood density values from repositories were relatively scarce and suffered from ambiguous or even missing method descriptions and were limited in species coverage resulting in seemingly arbitrary biomass over- and underestimations. The strong species-specific similarity in vertical basic wood

density trends are encouraging to develop correction equations relating basal basic wood density to that of the entire tree. For this to be effective in TLS inventories for AGB, more knowledge and data of basic wood density variation patterns are urgently needed.

Availability of data and materials The data that support the findings of this study are available upon reasonable request from the corresponding author MD.

Compliance with ethical standards

Conflict of interest The authors declare that they have no known competing financial interests or personal relationships that could have appeared to influence the work reported in this paper.

References

Alberti G, Candido P, Peressotti A, Turco S, Piussi P, Zerbi G (2005) Aboveground biomass relationships for mixed ash (*Fraxinus excelsior* L. and *Ulmus glabra* Hudson) stands in Eastern Prealps of Friuli Venezia Giulia (Italy). Ann For Sci 62:831–836. https://doi.org/10.1051/forest:2005089

Auty D, Achim A, Macdonald E, Cameron AD, Gardiner BA (2014) Models for predicting wood density variation in Scots pine. Forestry 87:449–458. https://doi.org/10.1093/forestry/cpu005

Barnett JR, Jeronimidis G (2003) Wood quality and its biological basis. Blackwell Publishing Ltd, Oxford

Bastin J-F, Fayolle A, Tarelkin Y, Van Den Bulcke J, De Haulleville T, Mortier F, Beeckman H, Van Acker J, Serckx A, Bogaert J, De Cannière C (2015) Wood specific gravity variations and biomass of central African tree species: the simple choice of the outer wood. PLoS ONE 10:1–16. https://doi.org/10.1371/journal.pone.0142146

Bastin J-F, Rutishauser E, Kellner JR, Saatchi S, Pélissier R, Hérault B, Slik F, Bogaert J, De Cannière C, Marshall AR, Poulsen J, Alvarez-Loyayza P, Andrade A, Angbonga-Basia A, Araujo-Murakami A, Arroyo L, Ayyappan N, de Azevedo CP, Banki O, Barbier N, Barroso JG, Beeckman H, Bitariho R, Boeckx P, Boehning-Gaese K, Brandão H, Brearley FQ, Breuer Ndoundou Hockemba M, Brienen R, Camargo JLC, Campos-Arceiz A, Cassart B, Chave J, Chazdon R, Chuyong G, Clark DB, Clark CJ, Condit R, Honorio Coronado EN, Davidar P, de Haulleville T, Descroix L, Doucet J-L, Dourdain A, Droissart V, Duncan T, Silva Espejo J, Espinosa S, Farwig N, Fayolle A, Feldpausch TR, Ferraz A, Fletcher C, Gajapersad K, Gillet J-F, Do-Amaral IL, Gonmadje C, Grogan J, Harris D, Herzog SK, Homeier J, Hubau W, Hubbell SP, Hufkens K, Hurtado J, Kamdem NG, Kearsley E, Kenfack D, Kessler M, Labrière N, Laumonier Y, Laurance S, Laurance WF, Lewis SL, Libalah MB, Ligot G, Lloyd J, Lovejoy TE, Malhi Y, Marimon BS, Marimon Junior BH, Martin EH, Matius P, Meyer V, Mendoza Bautista C, Monteagudo-Mendoza A, Mtui A, Neill D, Parada Gutierrez GA, Pardo G, Parren M, Parthasarathy N, Phillips OL, Pitman NCA, Ploton P, Ponette Q, Ramesh BR, Razafimahaimodison J-C, Réjou-Méchain M, Rolim SG, Saltos HR, Rossi LMB, Spironello WR, Rovero F, Saner P, Sasaki D, Schulze M, Silveira M, Singh J, Sist P, Sonke B, Soto JD, de Souza CR, Stropp J, Sullivan MJP, Swanepoel B, ter Steege H, Terborgh J, Texier N, Toma T, Valencia R, Valenzuela L, Ferreira LV, Valverde FC, Van Andel TR, Vasque R, Verbeeck H, Vivek P, Vleminckx J, Vos VA, Wagner FH, Warsudi PP, Wortel V, Zagt RJ, Zebaze D (2018) Pan-tropical prediction of forest structure from the largest trees. Glob Ecol Biogeogr. https://doi.org/10.1111/geb.12803

Bontemps JD, Gelhaye P, Nepveu G, Hervé JC (2013) When tree rings behave like foam: moderate historical decrease in the mean ring density of common beech paralleling a strong historical growth increase. Ann For Sci. https://doi.org/10.1007/s13595-013-0263-2

Bouriaud O, Bréda N, Le Moguédec G, Nepveu G (2004) Modelling variability of wood density in beech as affected by ring age, radial growth and climate. Trees Struct Funct 18:264–276. https://doi.org/10.1007/s00468-003-0303-x

Brus DJ, Hengeveld GM, Walvoort DJJ, Goedhart PW, Heidema AH, Nabuurs GJ, Gunia K (2012) Statistical mapping of tree species over Europe. Eur J For Res 131:145–157. https://doi.org/10.1007/s10342-011-0513-5

Burt A, Disney M, Calders K (2018) Extracting individual trees from lidar point clouds using treeseg. Methods Ecol Evol 2018:1–8. https://doi.org/10.1111/2041-210X.13121

Calders K, Newnham G, Burt A, Murphy S, Raumonen P, Herold M, Culvenor D, Avitabile V, Disney M, Armston J, Kaasalainen M (2015) Nondestructive estimates of above-ground biomass using terrestrial laser scanning. Methods Ecol Evol 6:198–208. https://doi.org/10.1111/2041-210X.12301

Calders K, Disney MI, Armston J, Burt A, Brede B, Origo N, Muir J, Nightingale J (2017) Evaluation of the range accuracy and the radiometric calibration of multiple terrestrial laser scanning

instruments for data interoperability. IEEE Trans Geosci Remote Sens 55:2716–2724. https://doi.org/10.1109/TGRS.2017.2652721

Calders K, Adams J, Armston J, Bartholomeus H, Bauwens S, Bentley LP, Chave J, Danson FM, Demol M, Disney M, Gaulton R, Krishna Moorthy SM, Levick SR, Saarinen N, Schaaf C, Stovall A, Terryn L, Wilkes P, Verbeeck H (2020) Terrestrial laser scanning in forest ecology: expanding the horizon. Remote Sens Environ 251:112102. https://doi.org/10.1016/j.rse.2020.112102

Campioli M, Malhi Y, Vicca S, Luyssaert S, Papale D, Peñuelas J, Reichstein M, Migliavacca M, Arain MA, Janssens IA (2016) Evaluating the convergence between eddy-covariance and biometric methods for assessing carbon budgets of forests. Nat Commun 7:1–12. https://doi.org/10.1038/ncomms13717

Cannell MGR, Morgan J (1989) Branch breakage under snow and ice loads. Tree Physiol. https://doi.org/10.1093/treephys/5.3.307

Chave J, Muller-Landau HC, Baker TR, Easdale TA, Hans Steege TER, Webb CO (2006) Regional and phylogenetic variation of wood density across 2456 neotropical tree species. Ecol Appl 16:2356–2367. https://doi.org/10.1890/1051-0761(2006)016[2356:RAPVOW]2.0.CO;2

Dassot M, Colin A, Santenoise P, Fournier M, Constant T (2012) Terrestrial laser scanning for measuring the solid wood volume, including branches, of adult standing trees in the forest environment. Comput Electron Agric 89:86–93. https://doi.org/10.1016/j.compag.2012.08.005

Dieter M, Elsasser P (2002) Kohlenstoffvorräte und - Veränderungen in der Biomasse der Waldbäume in Deutschland. Forstwissenschaftliches Cent 121:195–210. https://doi.org/10.1046/j.1439-0337.2002.02030.x

Disney MI, Boni Vicari M, Burt A, Calders K, Lewis SL, Raumonen P, Wilkes P (2018) Weighing trees with lasers: advances, challenges and opportunities. Interface Focus 8:20170048. https://doi.org/10.1098/rsfs.2017.0048

Falster DS, Duursma RA, Ishihara MI, Barneche DR, FitzJohn RG, Vårhammar A, Aiba M, Ando M, Anten N, Aspinwall MJ, Baltzer JL, Baraloto C, Battaglia M, Battles JJ, Bond-Lamberty B, van Breugel M, Camac J, Claveau Y, Coll L, Dannoura M, Delagrange S, Domec J-C, Fatemi F, Feng W, Gargaglione V, Goto Y, Hagihara A, Hall JS, Hamilton S, Harja D, Hiura T, Holdaway R, Hutley LS, Ichie T, Jokela EJ, Kantola A, Kelly JWG, Kenzo T, King D, Kloeppel BD, Kohyama T, Komiyama A, Laclau J-P, Lusk CH, Maguire DA, le Maire G, Mäkelä A, Markesteijn L, Marshall J, McCulloh K, Miyata I, Mokany K, Mori S, Myster RW, Nagano M, Naidu SL, Nouvellon Y, O'Grady AP, O'Hara KL, Ohtsuka T, Osada N, Osunkoya OO, Peri PL, Petritan AM, Poorter L, Portsmuth A, Potvin C, Ransijn J, Reid D, Ribeiro SC, Roberts SD, Rodríguez R, Saldaña-Acosta A, Santa-Regina I, Sasa K, Selaya NG, Sillett SC, Sterck F, Takagi K, Tange T, Tanouchi H, Tissue D, Umehara T, Utsugi H, Vadeboncoeur MA, Valladares F, Vanninen P, Wang JR, Wenk E, Williams R, de Aquino XF, Yamaba A, Yamada T, Yamakura T, Yanai RD, York RA (2015) BAAD: a biomass and allometry database for woody plants. Ecology 96:1445–1445. https://doi.org/10.1890/14-1889.1

Gonzalez de Tanago J, Lau A, Bartholomeus H, Herold M, Avitabile V, Raumonen P, Martius C, Goodman RC, Disney M, Manuri S, Burt A, Calders K (2018) Estimation of above-ground biomass of large tropical trees with terrestrial LiDAR. Methods Ecol Evol 9:223–234. https://doi.org/10.1111/2041-210X.12904

Hackenberg J, Spiecker H, Calders K, Disney M, Raumonen P (2015a) SimpleTree—an efficient open source tool to build tree models from TLS clouds. Forests 6:4245–4294. https://doi.org/10.3390/f6114245

Hackenberg J, Wassenberg M, Spiecker H, Sun D (2015b) Non destructive method for biomass prediction combining TLS derived tree volume and wood density. Forests 6:1274–1300. https://doi.org/10.3390/f6041274

Hakkila P (1967) Investigation on the basic density of Finnish pine, spruce and birch wood. Commun Inst For Fenn 61:98

Hosoi F, Nakai Y, Omasa K (2013) 3-D voxel-based solid modeling of a broad-leaved tree for accurate volume estimation using portable scanning lidar. ISPRS J Photogramm Remote Sens 82:41–48. https://doi.org/10.1016/j.isprsjprs.2013.04.011

Jackson T, Shenkin A, Wellpott A, Calders K, Origo N, Disney M, Burt A, Raumonen P, Gardiner B, Herold M, Fourcaud T, Malhi Y (2019) Finite element analysis of trees in the wind based on terrestrial laser scanning data. Agric For Meteorol 265:137–144. https://doi.org/10.1016/j.agrformet.2018.11.014

Janssens IA, Sampson DA, Cermak J, Meiresonne L, Riguzzi F, Overloop S, Ceulemans R (1999) Above- and belowground phytomass and carbon storage in a Belgian Scots pine stand. Ann For Sci 56:81–90. https://doi.org/10.1051/forest:19990201

Kankare V, Holopainen M, Vastaranta M, Puttonen E, Yu X, Hyyppä J, Vaaja M, Hyyppä H, Alho P (2013) Individual tree biomass estimation using terrestrial laser scanning. ISPRS J Photogramm Remote Sens 75:64–75. https://doi.org/10.1016/j.isprsjprs.2012.10.003

Karlman L, Mörling T, Martinsson O (2005) Wood density, annual ring width and latewood content in larch and scots pine. Eurasian J For Res 8:91–96

Kearsley E, De Haulleville T, Hufkens K, Kidimbu A, Toirambe B, Baert G, Huygens D, Kebede Y, Defourny P, Bogaert J, Beeckman H, Steppe K, Boeckx P, Verbeeck H (2013) Conventional tree height-diameter relationships significantly overestimate aboveground carbon stocks in the Central Congo Basin. Nat Commun. https://doi.org/10.1038/ncomms3269

Lachenbruch B, Moore JR, Evans R (2011) Radial variation in wood structure and function in woody plants, and hypotheses for its occurrence. Springer, Netherlands, pp 121–164

Lau A, Bentley LP, Martius C, Shenkin A, Bartholomeus H, Raumonen P, Malhi Y, Jackson T, Herold M (2018) Quantifying branch architecture of tropical trees using terrestrial LiDAR and 3D modelling. Trees Struct Funct 32:1219–1231. https://doi.org/10.1007/s00468-018-1704-1

Lau A, Calders K, Bartholomeus H, Martius C, Raumonen P, Herold M, Vicari M, Sukhdeo H, Singh J, Goodman RC (2019) Tree biomass equations from terrestrial LiDAR: a case study in Guyana. Forests. https://doi.org/10.3390/f10060527

Lavers GM, Moore GL (1983) The strength properties of timbers, 3rd edn. Dept. of the Environment, Building Research Establishment, London, Garston, Watford

Le Goff N, Granier A, Ottorini JM, Peiffer M (2004) Biomass increment and carbon balance of ash (Fraxinus excelsior) trees in an experimental stand in northeastern France. Ann For Sci 61:577–588. https://doi.org/10.1051/forest:2004053

Longuetaud F, Mothe F, Santenoise P, Diop N, Dlouha J, Fournier M, Deleuze C (2017) Patterns of within-stem variations in wood specific gravity and water content for five temperate tree species. Ann For Sci. https://doi.org/10.1007/s13595-017-0657-7

MacFarlane DW (2020) Functional relationships between branch and stem wood density for temperate tree species in North America. Front For Glob Chang 3:1–16. https://doi.org/10.3389/ffgc.2020.00063

Martínez-Sancho E, Slámová L, Morganti S, Grefen C, Carvalho B, Dauphin B, Rellstab C, Gugerli F, Opgenoorth L, Heer K, Knutzen F, von Arx G, Valladares F, Cavers S, Fady B, Alía R, Aravanopoulos F, Avanzi C, Bagnoli F, Barbas E, Bastien C, Benavides R, Bernier F, Bodineau G, Bastias CC, Charpentier JP, Climent JM, Corréard M, Courdier F, Danusevicius D, Farsakoglou AM, Del Barrio JMG, Gilg O, González-Martínez SC, Gray

A, Hartleitner C, Hurel A, Jouineau A, Kärkkäinen K, Kujala ST, Labriola M, Lascoux M, Lefebvre M, Lejeune V, Liesebach M, Malliarou E, Mariotte N, Matesanz S, Myking T, Notivol E, Pakull B, Piotti A, Pringarbe M, Pyhäjärvi T, Raffin A, Ramírez-Valiente JA, Ramskogler K, Robledo-Arnuncio JJ, Savolainen O, Schueler S, Semerikov V, Spanu I, Thévenet J, Mette Tollefsrud M, Turion N, Veisse D, Vendramin GG, Villar M, Westin J, Fonti P (2020) The GenTree Dendroecological collection, tree-ring and wood density data from seven tree species across Europe. Sci data 7:1. https://doi.org/10.1038/s41597-019-0340-y

Momo ST, Ploton P, Martin-Ducup O, Lehnebach R, Fortunel C, Sagang LBT, Boyemba F, Couteron P, Fayolle A, Libalah M, Loumeto J, Medjibe V, Ngomanda A, Obiang D, Pélissier R, Rossi V, Yongo O, Bocko Y, Fonton N, Kamdem N, Katembo J, Kondaoule HJ, Maïdou HM, Mankou G, Mbasi M, Mengui T, Mofack GII, Moundounga C, Moundounga Q, Nguimbous L, Ncham NN, Asue FOM, Senguela YP, Viard L, Zapfack L, Sonké B, Barbier N (2020) Leveraging signatures of plant functional strategies in wood density profiles of african trees to correct mass estimations from terrestrial laser data. Sci Rep 10:1–11. https://doi.org/10.1038/s41598-020-58733-w

Momo Takoudjou S, Ploton P, Sonké B, Hackenberg J, Griffon S, de Coligny F, Kamdem NG, Libalah M, Mofack GI, Le Moguédec G, Pélissier R, Barbier N (2017) Using terrestrial laser scanning data to estimate large tropical trees biomass and calibrate allometric models: a comparison with traditional destructive approach. Methods Ecol Evol. https://doi.org/10.1111/2041-210X.12933

Nogueira EM, Fearnside PM, Nelson BW (2008) Normalization of wood density in biomass estimates of Amazon forests. For Ecol Manage 256:990–996. https://doi.org/10.1016/j.foreco.2008.06.001

Pfeifer N, Gorte B, Winterhalder D (2004) Automatic reconstruction of single trees from terrestrial laser scanner data. Int Arch Photogramm Remote Sens Spat Inf Sci 35

R Development Core Team R (2011) R: a language and environment for statistical computing

Raumonen P, Kaasalainen M, Åkerblom M, Kaasalainen S, Kaartinen H, Vastaranta M, Holopainen M, Disney M, Lewis P (2013) Fast automatic precision tree models from terrestrial laser scanner data. Remote Sens 5:491–520. https://doi.org/10.3390/rs5020491

Repola J (2006) Models for vertical wood density of Scots pine, Norway spruce and birch stems, and their application to determine average wood density. Silva Fenn 40:673–685. https://doi.org/10.14214/sf.322

Saarinen N, Kankare V, Vastaranta M, Luoma V, Pyörälä J, Tanhuanpää T, Liang X, Kaartinen H, Kukko A, Jaakkola A, Yu X, Holopainen M, Hyyppä J (2017) Feasibility of Terrestrial laser scanning for collecting stem volume information from single trees. ISPRS J Photogramm Remote Sens 123:140–158. https://doi.org/10.1016/j.isprsjprs.2016.11.012

Sagang LBT, Momo Takoudjou S, Libalah MB, Rossi V, Fonton N, Mofack GI, Kamdem NG, Nguetsop VF, Sonké B, Ploton P, Barbier N (2018) Using volume-weighted average wood specific gravity of trees reduces bias in aboveground biomass predictions from forest volume data. For Ecol Manage 424:519–528. https://doi.org/10.1016/j.foreco.2018.04.054

Schauvliege M (1995) C-accumulatie in oude bestanden van het proefbos Aalmoeseneie. Master thesis, Universiteit Gent

Schüller E, Martínez-Ramos M, Hietz P (2013) Radial gradients in wood specific gravity, water and gas content in trees of a Mexican tropical rain forest. Biotropica 45:280–287. https://doi.org/10.1111/btp.12016

Schütt P, Schuck HJ, Aas G, Lang UM (1994) Enzyklopädie der Holzgewächse. Handbuch und Atlas der Dendrologie. Ecomed Verlagsgesellschaft, Landsberg am Lech

Somogyi Z, Cienciala E, Mäkipää R, Muukkonen P, Lehtonen A, Weiss P (2007) Indirect methods of large-scale forest biomass estimation. Eur J For Res 126:197–207. https://doi.org/10.1007/s10342-006-0125-7

Stephenson NL, Das AJ, Condit R, Russo SE, Baker PJ, Beckman NG, Coomes DA, Lines ER, Morris WK, Rüger N, Álvarez E, Blundo C, Bunyavejchewin S, Chuyong G, Davies SJ, Duque Á, Ewango CN, Flores O, Franklin JF, Grau HR, Hao Z, Harmon ME, Hubbell SP, Kenfack D, Lin Y, Makana JR, Malizia A, Malizia LR, Pabst RJ, Pongpattananurak N, Su SH, Sun IF, Tan S, Thomas D, Van Mantgem PJ, Wang X, Wiser SK, Zavala MA (2014) Rate of tree carbon accumulation increases continuously with tree size. Nature. https://doi.org/10.1038/nature12914

Stovall AEL, Vorster AG, Anderson RS, Evangelista PH, Shugart HH (2017) Non-destructive aboveground biomass estimation of coniferous trees using terrestrial LiDAR. Remote Sens Environ 200:31–42. https://doi.org/10.1016/j.rse.2017.08.013

Vallet P, Dhôte JF, Le MG, Ravart M, Pignard G (2006) Development of total aboveground volume equations for seven important forest tree species in France. For Ecol Manag 229:98–110. https://doi.org/10.1016/j.foreco.2006.03.013

Van den Bulcke J, Boone MA, Dhaene J, Van LD, Van HL, Boone MN, Wyffels F, Beeckman H, Van AJ, De Mil T (2019) Advanced X-ray CT scanning can boost tree-ring research for earth-system sciences. Ann Bot. https://doi.org/10.1093/aob/mcz126

Vande Walle I (2007) Carbon sequestration in short-rotation forestry plantations and in Belgian forest ecosystems. Doctoral thesis, Ghent University

Vande Walle I, Van Camp N, Perrin D, Lemeur R, Verheyen K, Van Wesemael B, Laitat E (2005) Growing stock-based assessment of the carbon stock in the Belgian forest biomass. Ann For Sci 62:853–864. https://doi.org/10.1051/forest:2005076

Vieilledent G, Fischer FJ, Chave J, Guibal D, Langbour P, Gérard J (2018) New formula and conversion factor to compute basic wood density of tree species using a global wood technology database. Am J Bot 105:1653–1661. https://doi.org/10.1002/ajb2.1175

Wagenführ R, Schreiber C (1985) Holzatlas. VEB Fachbuchverlag, Leipzig

Wahlgren HE, Fassnacht DL (1959) Estimating tree specific gravity from a single increment core. USDA For Serv For Prod Lab 24.

Wassenberg M, Chiu HS, Guo W, Spiecker H (2015) Analysis of wood density profiles of tree stems: incorporating vertical variations to optimize wood sampling strategies for density and biomass estimations. Trees Struct Funct 29:551–561. https://doi.org/10.1007/s00468-014-1134-7

Wiemann MC, Williamson GB (2012) Testing a novel method to approximate wood specific gravity of trees. For Sci 58:577–591. https://doi.org/10.5849/forsci.10-049

Wiemann MC, Williamson GB (2014) Wood Specific Gravity Variation with Height and Its Implications for Biomass Estimation

Wilkes P, Lau A, Disney M, Calders K, Burt A, Gonzalez de Tanago J, Bartholomeus H, Brede B, Herold M (2017) Data acquisition considerations for Terrestrial Laser Scanning of forest plots. Remote Sens Environ 196:140–153. https://doi.org/10.1016/j.rse.2017.04.030

Williamson GB, Wiemann MC (2010) Measuring wood specific gravity...correctly. Am J Bot 97:519–524. https://doi.org/10.3732/ajb.0900243

Zanne AE, Lopez-Gonzalez G, Coomes DAA, Ilic J, Jansen S, Lewis SLSL, Miller RBB, Swenson NGG, Wiemann MCC, Chave J (2009) Dat from: towards a worldwide wood economics spectrum. Dryad Dig Repos Dryad 235:33. https://doi.org/10.5061/dryad.234